Novel Oxygen-Containing π-Electron Donors for Organic Metals: 2-(1,3-Dithiol-2-ylidene)-5-(pyran-4-ylidene)-1,3,4,6-tetrathiapentalenes

Yohji Misaki,*,† Hideki Fujiwara,† Takashi Maruyama,† Masateru Taniguchi,† Tokio Yamabe,† Takehiko Mori,‡ Hatsumi Mori,§ and Shoji Tanaka§

Department of Molecular Engineering, Graduate School of Engineering, Kyoto University, Yoshida, Kyoto 606-8501, Japan, Department of Organic and Polymeric Materials, Faculty of Engineering, Tokyo Institute of Technology, O-okayama, Tokyo 152-8552, Japan, and International Superconductivity Technology Center, Shinonome, Tokyo 135-0062, Japan

Received October 28, 1998. Revised Manuscript Received May 20, 1999

A bis-fused π-electron donor incorporating a pyran-4-ylidene moiety, 2-(1,3-dithiol-2-ylidene)-5-(pyran-4-ylidene)-1,3,4,6-tetrathiapentalene (PDT−TTP, **1a**), and its derivatives (**1b**−**d**) have been synthesized. The cyclic voltammograms of PDT−TTPs are composed of three pairs of redox waves. Comparison of the first oxidation potentials (E_1) suggests PDT−TTP (+0.42 V vs SCE in benzonitrile) is a weaker donor than TTF (+0.35 V). The present donors have produced a large number of highly conducting ($\sigma_{rt} = 10^0-10^2$ S cm^{-1}) molecular complexes. Among them, conducting salts based on the ET−PDT (**1d**) are metallic down to liquid helium temperature. The metallic PF_6^- salt of ET−PDT has a composition of (ET−PDT)$_4$PF$_6$(cn), where cn is 1-chloronaphthalene, in which two crystallographically independent ET−PDT molecules A and B form a face-to-face stack with a four-folded period as A′ABB′. In the present salt, the head-to-tail overlap of the unsymmetrical π-electron framework of PDT−TTP prevents an effective intrastack overlap and produces a strongly dimerized electronic structure along the stack direction. Tight-binding band calculations indicate that it has opened Fermi surfaces characteristic of quasi-one-dimensional metals.

Introduction

Since the discovery of the first organic metal in the tetrathiafulvalene−tetracyano-*p*-quinodimethane (TTF−TCNQ) complex,[1] much interest has been focused on the organic conductors in various scientific fields, including organic and physical chemistry, solid-state physics, and material science.[2−4] In particular, discoveries of superconductivity in the cation radical salts based on first tetramethyltetraselenafulvalene (TMTSF)[5] and subsequently bis(ethylenedithio)−TTF (BEDT−TTF)[6] have stimulated considerable attention for the development of new π-electron donors. Up to now, a large number of TTF and TSF derivatives, extended TTFs, and TTF dimers have been synthesized.[7] Among them, one of the most attractive TTF families is bis(ethylenedioxy)−TTF (BEDO−TTF),[8,9] the first oxygen-substituted TTF developed by Wudl et al.[8] because it has afforded superconducting $Cu_2(NCS)_3^-$ [10] and ReO_4^- [11] salts as well as a great number of metallic salts stable down to liquid helium temperatures.[9] To develop new oxygen-based donors, various TTF derivatives substituted with eth-

† Kyoto University.
‡ Tokyo Institute of Technology.
§ International Superconductivity Technology Center.

(1) Ferraris, J.; Cowan, D. O.; Walatka, V., Jr.; Perlstein, J. H. *J. Am. Chem. Soc.* **1973**, *95*, 948−949.

(2) Recent Proceedings of the International Conferences: (a) Proceedings of the International Conference on Science and Technology of Synthetic Metals, Snowbird, UT. Vardeny, Z. V.; Epstein, A. J.; Eds. *Synth. Met.* **1997**, *84*−*86*. (b) Proceedings of the Symposium on Advances in the Chemistry and Physics of Novel Low-Dimensional and Conducting or Superconducting Solids, Honolulu, HI. Williams, J. M., Geiser, U., Mori, T., Eldridge, J. E., Eds. *Mol. Cryst. Liq. Cryst.* **1996**, *284*.

(3) (a) Williams, J. M.; Ferraro, J. R.; Thorn, R. J.; Carlson, K. D.; Geiser, U.; Wang, H. H.; Kini, A. M.; Whangbo, M.-H. *Organic Superconductors*; Prentice Hall: Englewood Cliffs, NJ, 1992. (b) Ishiguro T.; Yamaji, K. *Organic Superconductors*; Springer-Verlag: Berlin, Heidelberg, Germany, 1990.

(4) Reviews: (a) Bechgaard, K.; Jérome, D. *Sci. Am.* **1982**, *247*, 50−59. (b) Williams, J. M.; Schultz, A. J.; Geiser, U.; Carlson, K. D.; Kini, A. M.; Wang, H. H.; Kwok, W. K.; Whangbo, M.-H.; Schirber, J. E. *Science* **1991**, *252*, 1501−1508. (c) Saito, G. *Phosphorus, Sulfur, Silicon* **1992**, *67*, 345−360.

(5) (a) Jérome, D.; Mazaud, A.; Ribault, M.; Bechgaard, K. *J. Phys. Lett.* **1980**, *41*, L95−98. (b) Bechgaard, K.; Jacobsen, C. S.; Mortensen, K.; Pedersen, H. J.; Thorup, N. *Solid State Commun.* **1980**, *33*, 1119−1125. (c) Bechgaard, K.; Carneiro, K.; Rasmussen, F. B.; Olsen, M.; Rindorf, G.; Jacobsen, C. S.; Pedersen, H. J.; Scott, J. C. *J. Am. Chem. Soc.* **1981**, *103*, 2440−2442.

(6) (a) Parkin, S. S. P.; Engler, E. M.; Schumaker, R. R.; Lagier, R.; Lee, V. Y.; Scott, J. C.; Greene, R. L. *Phys. Rev. Lett.* **1983**, *50*, 270−273. (b) Yagubskii, E. B.; Schegolev, I. F.; Laukhin, V. N.; Kononovich, P. A.; Karatsovnik, M. V.; Zvarykina, A. V.; Buravov, L. I. *Pis'ma Zh. Eksp. Teor. Fiz.* **1984**, *39*, 12−15; *JETP. Lett. (Engl. Transl.)* **1984**, *39*, 12−16.

(7) Reviews: (a) Krief, A. *Tetrahedron* **1986**, *42*, 1209−1252. (b) Adam, M.; Müllen, K. *Adv. Mater.* **1994**, *6*, 439−459. (c) Bryce, M. R. *J. Mater. Chem.* **1995**, *5*, 1481−1496. (d) Otsubo, T.; Aso, Y.; Takimiya, K. *Adv. Mater.* **1996**, *8*, 203-211.

(8) Suzuki, T.; Yamochi, H.; Srdanov, G.; Hinkelmann, K.; Wudl, F. *J. Am. Chem. Soc.* **1989**, *111*, 3108−3109.

(9) (a) Wudl, F.; Yamochi, H.; Suzuki, T.; Isotalo, H.; Fite, C.; Kasmai, H.; Liou, K.; Srdanov, G.; Coppens, P.; Maly K.; Frost-Jensen, A. *J. Am. Chem. Soc.* **1990**, *112*, 2461−2462. (b) Beno, M. A.; Wang, H. H.; Carlson, K. D.; Kini, A. M.; Frankenbach, G. M.; Ferraro, J. R.; Larson, N.; McCabe, G. D.; Thompson, J.; Purnama, C.; Vashon, M.; Williams, J. M.; Jung D.; Whangbo, M.-H. *Mol. Cryst. Liq. Cryst.* **1990**, *181*, 145−159. (c) Horiuchi, S.; Yamochi, H.; Saito, G.; Sakaguchi, K.; Kusunoki, M. *J. Am. Chem. Soc.* **1996**, *118*, 8604−8622.

10.1021/cm981035p CCC: $18.00
Published on Web 07/31/1999

ylenedioxy,[12] ethyleneoxythio,[13] and methoxy[14] groups have been also prepared so far. Conducting materials based on tetraoxafulvalene (TOF) are also desirable. Though the synthesis of the dibenzo derivatives of TOF[15] and oxatrithiafulvalene[16] have been reported so far, no solid-state property of molecular complexes based on these donors has been described. In this connection, the development of organic metals based on alternative oxygen-containing π-electron frameworks is of interest. Bi(pyran-4-ylidene) (BP) and 1,6-dioxapyrane (DOP) are representatives of such donors. The synthesis of BP and its derivatives have been already reported in early 1970s,[17] however, there is no example of metal-like conducting compound based on BP donors. On the other hand, DOP and its derivatives have been recently synthesized by two independent groups,[18] and the BF_4^- and PF_6^- salts of 3,5,8,10-tetramethyl-DOP have been found to show semiconductive behavior with high conductivity ($\sigma_{rt} = 30$ S cm^{-1} for the BF_4^- salt).[19] Both DOP and BP donors unfortunately have one disadvantage for their use in the preparation of organic metals stable down to low temperatures, namely, no expectation for realization of the two-dimensional property through a transverse chalcogen−chalcogen interaction in both systems owing to the lack of a ladderlike array of chalcogen atoms as is observed in BEDO−TTF systems. To stabilize the metallic state of cation radical salts, a fusion of 1,3-dithiole donors, in other words, an insertion of a tetrathiapentalene moiety, is a promising strategy.[20−22] In fact, bis-fused TTF, 2,5-bis(1,3-dithiol-2-ylidene)-1,3,4,6-tetrathiapentalene (TTP), has produced many metallic cation radical salts stable down to 0.6−1.2 K.[21] Furthermore we have recently found that a vinyl analogue of TTP, 2-(1,3-dithiol-2-ylidene)-5-(2-ethanediylidene-1,3-dithiole)-1,3,4,6-tetrathiapentalene (DTEDT), has afforded a superconducting $Au(CN)_2^-$ salt ($T_c = 4$ K under ambient pressure).[22] In this article we describe the synthesis, structures and properties of the first TTP−BP hybrid system, 2-(1,3-dithiol-2-ylidene)-5-(pyran-4-ylidene)-1,3,4,6-tetrathiapentalene (PDT−TTP) derivatives (**1a**−**d**; Chart 1),[23] and their charge-transfer salts.

Chart 1

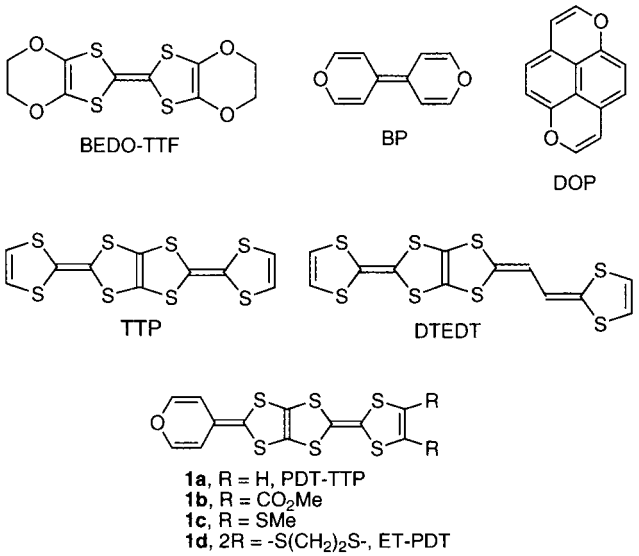

Chart 2

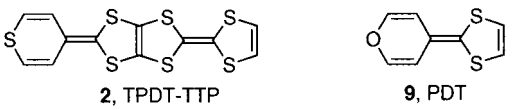

Results and Discussion

Synthesis. Synthesis of PDT−TTPs was achieved by use of a synthetic method similar to that used for a thiopyran analogue, TPDT−TTP (**2**; Chart 2), as shown in Scheme 1.[24] A phosphorus reagent, **3**,[25] was treated with an equimolar amount of lithium diisopropylamide (LDA) in THF at −78 °C in the presence of tetrahydropyran-4-one (**4**) to give a 1,3-dithiole-2-thione fused with 2-tetrahydropyran-4′-ylidene-1,3-dithiole (**5**) in 86% yield. Thione **5** was converted into the corresponding ketone (**6**) by the treatment with an excess of mercury(II) acetate in chloroform−acetic acid (3:1, v/v) at room temperature (91% yield). By the cross-coupling reaction of **6** with 1,3-dithiole-2-thiones (**7b**−**d**) in neat triethyl phosphite at 80 °C were obtained the corresponding tetrahydro derivatives of **1** (**8b**−**d**) in 50−87% yields. Dehydrogenation of **8b**−**d** with a slight excess (2.8 mol equiv) of 2,3-dichloro-5,6-dicyano-*p*-benzoquinone (DDQ) in refluxing xylene efficiently proceeds without any

(10) Beno, M. A.; Wang, H. H.; Kini, A. M.; Carlson, K. D.; Geiser, U.; Kwok, W. K.; Thompson, J. E.; Williams, J. M.; Ren, J.; Whangbo, M.-H. *Inorg. Chem.* **1990**, *29*, 1599−1601.
(11) Kahlich, S.; Schweitzer, D.; Heinen, I.; Lan, S. E.; Nuber, B.; Keller, H. J.; Winzer, K.; Helberg, H. W. *Solid State Commun.* **1991**, *80*, 191−195.
(12) (a) Kini, A. M.; Mori, T.; Geiser, U.; Budz, S. M.; Williams, J. M. *J. Chem. Soc., Chem. Commun.* **1990**, 647−648. (b) Mori, T.; Inokuchi, H.; Kini, A. M.; Williams, J. M. *Chem. Lett.* **1990**, 1279−1282. (c) Papavassiliou, G. C.; Kakoussis, V. C.; Lagouvardos D. J.; Mousdis, G. A. *Mol. Cryst. Liq. Cryst.* **1990**, *181*, 171−184. (d) Fabre, J. M.; Serhani, D.; Saoud, K.; Chakroune, S.; Hoch, M. *Synth. Met.* **1993**, *60*, 295−298. (e) Imakubo, T.; Okano, Y.; Sawa, H.; Kato, R. *J. Chem. Soc., Chem. Commun.* **1995**, 2493−2494. (f) Yamada, J.; Tanaka, S.; Anzai, H.; Sato, T.; Nishikawa, H.; Ikemoto, I.; Kikuchi, K. *J. Mater. Chem.* **1997**, *7*, 1311−1312. (g) Imakubo, T.; Kobayashi, K. *J. Mater. Chem.* **1998**, *8*, 1945−1947.
(13) Hellberg, J.; Moge, M.; Bauer, D.; von Schütz, J.-U. *J. Chem. Soc., Chem. Commun.* **1994**, 817−818.
(14) Misaki, Y.; Nishikawa, H.; Nomura, K.; Yamabe, T.; Yamochi, H.; Saito, G. *J. Chem. Soc., Chem. Commun.* **1992**, 1410−1411.
(15) Safiev, O. G.; Nazarov, D. V.; Zorin, V. L.; Rakhmankulov, D. L. *Khim. Geterotsikl. Soedin.* **1988**, *6*, 852−852.
(16) D'Arcangelis, S. T.; Cowan, D. O. *Tetrahedron Lett.* **1996**, *37*, 2931−2934.
(17) Hünig, S.; Garner, B. J.; Ruider, G.; Schenk, W. *Liebigs Ann. Chem.* **1973**, 1036−1060.
(18) (a) Buisson, J.-P.; Demerseman, P. *J. Heterocycl. Chem.* **1990**, *27*, 2213−2214. (b) Bechgaard, K.; Lerstrup, K.; Jørgensen M.; Johannsen, I.; Christensen, J.; Larsen J. *Mol. Cryst. Liq. Cryst.* **1990**, *181*, 161−169. (c) Christensen, J. B.; Larsen J.; Johannsen, I.; Bechgaard, K. *Synth. Met.* **1991**, *42*, 2311−2313. (d) Christensen, J. B.; Johannsen, I.; Bechgaard, K. *J. Org. Chem.* **1991**, *56*, 7055−7058.
(19) Thorup, N.; Hjorth, M.; Christensen, J. B.; Bechgaard, K. *Synth. Met.* **1993**, *56*, 2069−2072.
(20) (a) Misaki, Y.; Nishikawa, H.; Kawakami, K.; Koyanagi, S.; Yamabe, T.; Shiro, M. *Chem. Lett.* **1992**, 2321−2324. (b) Misaki, Y.; Matsui, T.; Kawakami, K.; Nishikawa, H.; Yamabe, T.; Shiro, M. *Chem. Lett.* **1993**, 1337−1340.
(21) (a) Misaki, Y.; Fujiwara, H.; Yamabe, T.; Mori, T.; Mori, H.; Tanaka, S. *Chem. Lett.* **1994**, 1653−1656. (b) Mori, T.; Misaki, Y.; Fujiwara, H.; Yamabe, T. *Bull. Chem. Soc. Jpn.* **1994**, *67*, 2685−2689.
(22) Misaki, Y.; Higuchi, N.; Fujiwara, H.; Yamabe, T.; Mori, T.; Mori, H.; Tanaka, S. *Angew. Chem., Int. Ed. Engl.* **1995**, *34*, 1222−1225.
(23) A part of the result has been reported as preliminary proceedings: Misaki, Y.; Fujiwara, H.; Maruyama, T.; Yamabe, T. *Synth. Met.* **1995**, *70*, 1147−1148.
(24) Misaki, Y.; Fujiwara, H.; Yamabe, T. *J. Org. Chem.* **1996**, *61*, 3650−3656.
(25) Misaki, Y.; Nishikawa, H.; Kawakami, K.; Uehara, T.; Yamabe, T. *Tetrahedron Lett.* **1992**, *33*, 4321−4324.

Scheme 1[a]

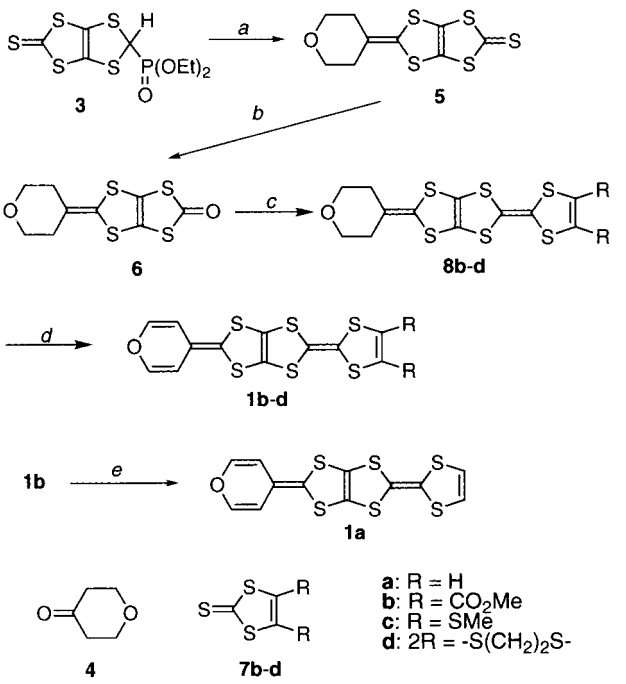

[a] Key: (a) compound **4**, LDA (1 equiv), THF, −78 °C, 20 min (86%); (b) $Hg(OAc)_2$, $CHCl_3$−AcOH (3:1, v/v), room temperature, 2 h (91%); (c) compounds **7b**−**d** (2 equiv), $P(OEt)_3$, 80 °C, 2 h (50−87%); (d) DDQ (2.8 equiv), xylene, reflux, 40 min (59−90%); (e) $LiBr·H_2O$ (10 equiv), HMPA, 90 °C, 1 h, 110 °C, 40 min (88%).

formation of the charge-transfer complexes to give the target molecules **1b**−**d** in 59−90% yields. The unsubstituted PDT−TTP (**1a**) was obtained in 88% yield by the demethoxycarbonylation of **1b** with an excess (10 mol equiv) of $LiBr·H_2O$ in hexamethylphosphoramide (HMPA) at 90 °C and then at 110 °C.[26] All donors are stable solids and are considerably less soluble compared to the corresponding TTF derivatives and 2-(pyran-4-ylidene)-1,3-dithiole (**9**; Chart 2).[27]

Electrochemical Properties. The electrochemical properties of new donors **1a,c** were investigated by cyclic voltammetry.[28] Both donors display three pairs of redox waves, and the peak current of the redox wave in the highest potential region is about twice as large as the other ones. Considering that there are four redox-active sites (one pyran-4-ylidene and three 1,3-dithiol-2-ylidenes), we have concluded that the third wave corresponds to the double-electron-transfer process. It is in contrast to the redox behavior of TPDT−TTP, **2**, which shows four pairs of single-electron redox waves.[25] Their redox potentials are summarized in Table 1 together with those of the related compounds. The first oxidation potential (E_1) of **1a** (+0.42 V vs SCE) is higher by 0.07−0.13 V than those of TTF (+0.35 V) and **9** (+0.29 V). The increase of the E_1 value by the fusion of two donor units is a common feature of the bis-fused π-electron donors.[21b,25,29] On the other hand, the E_1 value of **1a** is higher by ca. 0.05 V than that of **2**, suggesting that the donating ability decreases by the replacement of sulfur atoms in the thiopyran ring with oxygen atom. The $E_2 - E_1$ value of **1a** (0.21 V) is smaller by ca. 0.2 V than those of TTF (0.42 V) and **9** (0.44 V), and comparable to that of **2** (0.23 V). This result strongly indicates that the on-site Coulomb repulsion in the dication of PDT−TTP considerably decreases compared to those of TTF and **9** due to the delocalization of two positive charges over two donor units.

Table 1. Redox Potentials of PDT−TTP Derivatives 1 and Their Related Compounds in PhCN (V vs SCE, 25 °C)

compound	E_1	E_2	E_3	E_m	E_4[b]	$E_2 - E_1$
1a	+0.42	+0.63		+1.07[b]		0.21
1c	+0.44	+0.68		+1.07[b]		0.24
2	+0.37	+0.60	+0.94		+1.11	0.23
TTF	+0.35	+0.77				0.42
9	+0.29	+0.73				0.44

[a] $E_m = (E_3 + E_4)/2$. [b] Irreversible step. Anodic peak potential.

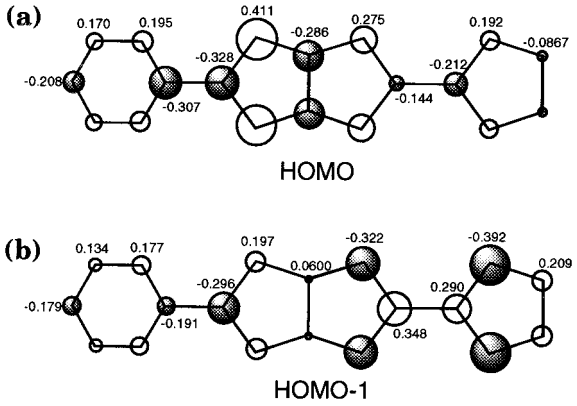

Figure 1. Atomic coefficients of PDT−TTP in the HOMO (a) and in the HOMO-1 (b). The radii of the circles are approximately proportional to the LCAO coefficients.

Molecular Orbital Calculation. The molecular orbital calculation for PDT−TTP was performed based on a semiempirical MNDO method by using the Gaussian 90 program.[30] The geometry was fully optimized supposing C_{2v} symmetry. Figure 1 shows the highest occupied molecular orbital (HOMO) and the second HOMO (HOMO-1) of PDT−TTP. The HOMO of PDT−TTP is constructed from the in-phase interaction between those of each TTF[31] and PDT units. In contrast, HOMO-1 consists of the HOMOs of TTF and PDT which interact out-of-phase with each other and has a node at the central C=C double bond of the tetrathiapentalene moiety. In the HOMO of PDT−TTP, all sulfur atoms in the 1,3-dithiole rings possess the same phase. This situation indicates the expectation of an effective transverse intermolecular interaction in the cation radical salts, which is an indispensable requirement for the

(26) (a) Lakshmikantham, M. V.; Cava, M. P. *J. Org. Chem.* **1976**, *41*, 882. (a) Sandman, D. J.; Fisher, A. P., III; Holmes, T. J.; Epstein, A. J. *J. Chem. Soc., Chem. Commun.* **1977**, 687−688. (c) Yoneda, S.; Kawase, T.; Yasuda, Y.; Yoshida, Z. *J. Org. Chem.* **1979**, *44*, 1728−1729. (d) Sugimoto, T.; Awaji, H.; Sugimoto, I.; Misaki, Y.; Kawase, T.; Yoneda, S.; Yoshida, Z.; Kobayashi, T.; Anzai, H. *Chem. Mater.* **1989**, *1*, 535−547.

(27) Misaki, Y.; Fujiwara, H.; Maruyama, T.; Yamabe, T. Unpublished results.

(28) Satisfactory voltammograms could not be obtained for the bis(methoxycarbonyl) and ethylenedithio derivatives **1b,d** owing to their extremely low solubility in the common solvents.

(29) Misaki, Y.; Ohta, T.; Higuchi, N.; Fujiwara, H.; Yamabe, T.; Mori, T.; Mori, H.; Tanaka, S. *J. Mater. Chem.* **1995**, *5*, 1571−1579.

(30) Frisch, M. J.; Head-Gordon, M.; Trucks, G. W.; Foresman, J. B.; Schlegel, H. B.; Defrees, D. J.; Fox, D. J.; Whiteside, R. A.; Seeger, R.; Melius, C. F.; Baker, J.; Martin, R. L.; Kahn, L. R.; Stewart, J. J. P.; Topiol, S.; Pople, J. A. *Gaussian 90, Revision F*; Gaussian, Inc: Pittsburgh, PA, 1990.

(31) Bøwadt, S.; Jensen, F. *Synth. Met.* **1989**, *32*, 179−190.

Table 2. Electrical Properties of TCNQ Complexes and Cation Radical Salts Based on PDT−TTP Derivatives (Donor·(A)$_x$)

donor	acceptor	solvent[a]	form[b]	x[c]	σ_{rt}, S cm^{-1}[d]	conducting behavior
1a	TCNQ	PhCl		0.75	30[e]	T_{MI} = 200 K
	ClO_4^-	DCE	P	0.36 (Cl)	2	E_a = 0.030 eV
	PF_6^-	PhCl	P	0.38 (P)	5	E_a = 0.029 eV
	I_3^-	PhCl		0.5	2[e]	E_a = 0.030 eV
1c	TCNQ	PhCl		1.0	9[e]	E_a = 0.011 eV
	ClO_4^-	PhCl	N	0.5	100	T_{MI} = 125 K
	BF_4^-	PhCl	N	0.6	20	E_a = 0.046 eV
	ReO_4^-	PhCl	N	0.5	20	T_{MI} = 240 K
	PF_6^-	PhCl	N	0.5	70	T_{MI} = 200 K
	AsF_6^-	PhCl	N	0.5	40	T_{MI} = 230 K
	SbF_6^-	PhCl	N	0.5	4	T_{MI} = 280 K
	I_3^-	PhCl		0.5	0.4[e]	E_a = 0.070 eV
1d	TCNQ	PhCl	N	1.0	80	*M* down to 4.2 K[f]
	PF_6^-	cn/DCE	P	0.25[g]	50	*M* down to 4.2 K[f]
	AsF_6^-	cn/DCE	P	0.42 (As)[h]	50	*M* down to 1.5 K[f]
	SbF_6^-	cn/DCE	P	0.21 (Sb)[h]	70	*M* down to 1.5 K[f]
	TaF_6^-	cn/DCE	P	0.31 (Ta)[h]	30	*M* down to 4.2 K[f]
	I_3^-	PhCl		0.4 (I)[h]	2	*M* down to 4.2 K[f]
	$Au(CN)_2^-$	cn/DCE	P	0.32 (Au)[h]	30	*M* down to 4.2 K[f]

[a] DCE = 1,2-dichloroethane, cn = 1-chloronaphthalene. [b] N = needle, P = plate. [c] Determined based on elemental analyses. [d] Room temperature conductivity measured on a single crystal using the four-probe technique. [e] Measured on a compressed pellet. [f] M designates metallic behavior. [g] Determined based on X-ray structure analysis. [h] Determined by the energy dispersion spectroscopy (EDS) from the ratio of sulfur and the elements designated in the parentheses.

realization of two-dimensional electronic structures.[32] The atomic coefficient of oxygen atom is a little smaller than that of sulfur atom in TPDT−TTP, but has a still relatively large value of 0.208. Therefore, three-dimensionality based on the inter donor layer interactions may be enhanced through the oxygen−oxygen interactions compared with BEDT−TTF salts if the interlayer oxygen−oxygen distances are short enough.

Preparation and Electrical Properties of Charge-Transfer Complexes and Cation Radical Salts. All the PDT−TTP donors except for the bis(methoxycarbonyl) derivative reacted with tetracyano-*p*-quinodimethane (TCNQ) and tetra-*n*-butylammonium triiodide to give the corresponding TCNQ complexes and I_3^- salts. The other cation radical salts were electrochemically prepared by use of a controlled current technique.[33] Their electrical properties are summarized in Table 2. The room-temperature conductivity of **1a**·TCNQ (30 S cm^{-1}) is comparable to that of **2**·TCNQ (40 S cm^{-1}).[25] It showed the metallic temperature dependence of resistivity down to 200 K despite the fact that the measurement was achieved on a compressed pellet, while **2**·TCNQ was a semiconductor under similar conditions. In contrast, all the cation radical salts of **1a** with inorganic acceptors obtained so far were semiconductors, though the conductivity measurement of the ClO_4^- and PF_6^- salts was performed on single crystals.

The bis(methylthio) derivative **1c** gave highly conducting (10^{-1}−10^0 S cm^{-1} on a compressed pellet) TCNQ and I_3^- salts, both of which are semiconductors with small activation energies (E_a = 0.011−0.07 eV). On the other hand, the cation radical salts with several tetrahedral and octahedral anions were obtained as single crystals. Most of them showed metallic conducting behavior, though the degree of temperature dependence

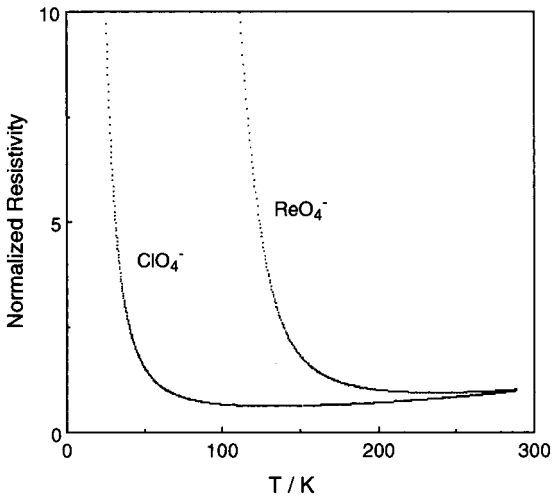

Figure 2. Conducting behavior of the metallic cation radical salts of **1c**.

is weak (Figure 2). All the metallic salts were subject to the metal to semiconductor transition at 125−280 K, probably owing to one-dimensional instability, considering that the methylthio groups often prevent the side-by-side interactions by projecting them outside of the molecular long axis.[34] There is a tendency that the T_{MI} rises as the size of the anions increases. Such destabilization of the metallic state in the salts with larger anions is possibly due to the formation of a larger intrastack space and the resulting narrower bandwidth.

The ethylenedithio derivative **1d** formed single crystals with TCNQ and several inorganic anions. All of them displayed a high conductivity of $\sigma_{rt} = 10^1$ S cm^{-1} and metallic conducting behavior down to 1.5−4.2 K. It is remarkable that this donor affords metallic salts with various acceptors of octahedral and linear inor-

(32) (a) Mori, T.; Inokuchi, H.; Misaki, Y.; Fujiwara, H.; Yamabe, T.; Mori, H.; Tanaka, S. *Chem. Lett.* **1993**, 733−736. (b) Mori, T.; Kawamoto, T.; Misaki, Y.; Kawakami, K.; Fujiwara, H.; Yamabe, T.; Mori, H.; Tanaka, S. *Mol. Cryst. Liq. Cryst.* **1996**, *284*, 271−282.

(33) Anzai, H.; Delrieu, J. M.; Takasaki, S.; Nakatsuji, S.; Yamada, J. *J. Cryst. Growth* **1995**, *154*, 145−150.

(34) (a) Katayama, C.; Honda, M.; Kumagai, H.; Tanaka, J.; Saito, G.; Inokuchi, H. *Bull. Chem. Soc. Jpn.* **1985**, *58*, 2272−2278. (b) Wu, P.; Mori, T.; Enoki, T.; Imaeda, K.; Saito, G.; Inokuchi, H.; *Bull. Chem. Soc. Jpn.* **1986**, *59*, 127−132. (c) Mori, T.; Inokuchi, H.; Misaki, Y.; Yamabe, T.; Mori, H.; Tanaka, S. *Bull. Chem. Soc. Jpn.* **1994**, *67*, 661−667.

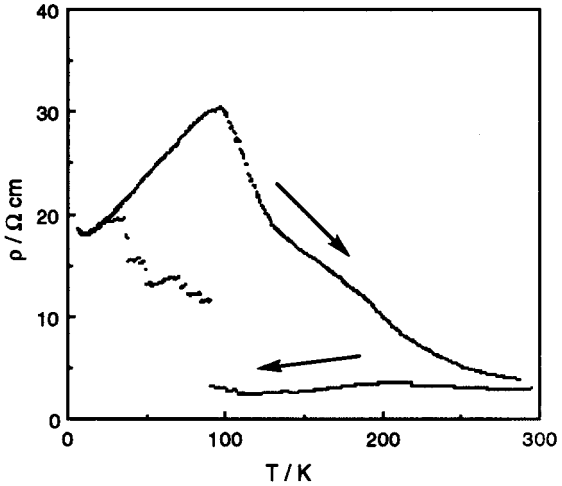

Figure 3. Conducting behavior of the PF_6^- salt of **1d**.

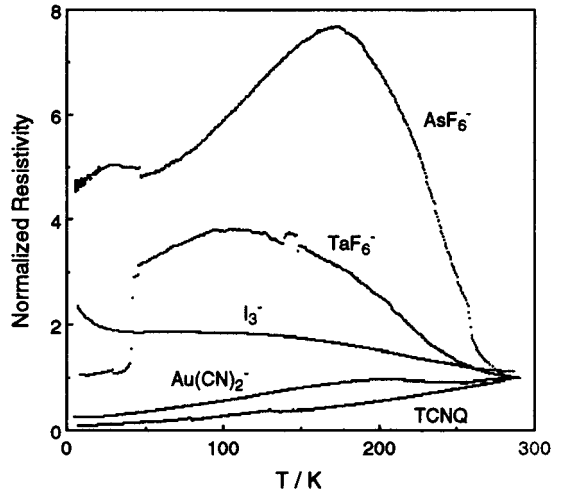

Figure 4. Conducting behavior of the metallic cation radical salts of **1d** in the heating run.

ganic ones and TCNQ. In contrast, the corresponding sulfur analogue, ethylenedithio−TPDT−TTP gave no metallic salt down to low temperatures; in particular, octahedral anions yielded only low conductive ($\sigma_{rt} = 10^{-2}$ S cm^{-1}) semiconductors with large activation energy (E_a > 0.1 eV), probably due to differences of their crystal structure in comparison to that of **1d**, assumed from the differences of crystal shapes. Figure 3 shows the conducting behavior of the PF_6^- salt. In the cooling run, it showed a simple metallic temperature dependence down to ca. 90 K. Then the resistivity increased a little with several jumps below 100 K but decreased again below ca. 40 K. In the heating run, this salt showed a resistivity hump around 100 K. Such a conducting behavior is probably due to the formation of microcracks during the cooling process. A similar temperature dependence was observed for the other **1d** salts with octahedral anions (Figure 4). In contrast to octahedral anions, a linear anion, $Au(CN)_2^-$, and an organic acceptor, TCNQ, afford organic metals showing simple temperature dependence though ρ_{rt}/ρ_{min} (4−10) is not so large (see also Figure 4). On the other hand, a compressed pellet of (**1d**)$(I_3)_{0.4}$ also showed metallike temperature dependence, and the resistivity minimum was about 200 K. Because the increase of resistivity below this temperature is very small and did not obey a semiconductive temperature dependence, this salt should be essentially metallic down to 4.2 K, and the increase of resistivity is due to the measurement on a compressed pellet.

Crystal and Electronic Structures of (ET−PDT)$_4$PF$_6$(cn) (cn = 1-Chloronaphthalene). Among the cation radical salts obtained so far, the PF_6^- salt of ET−PDT (**1d**) had a good enough quality for use in an X-ray structure analysis. There are two kinds of crystallographically independent donor molecules (molecules A and B) in the unit cell, and the PF_6^- anion lies on a center of inversion. The unit cell also includes one 1-chloronaphthalene molecule used as a solvent for the electrocrystallization. Though 1-chloronaphthalene has a noncentrosymmetric structure, it is also located on a center of inversion due to a positional disorder of the chlorine atom. Because the population analysis indicated no significant lack of a phosphorus atom, the composition of the present salt was determined to be (ET−PDT)$_4$PF$_6$(cn). Figure 5 shows molecular structures and atomic numbering schemes of the donors A and B. The PDT−TTP skeletons of both molecules A and B are almost planar, and their molecular structures are very close to each other. The deviation from the optimal planes are 0.047 Å for A and 0.026 Å for B, respectively. Their bond lengths are little different from each other within the experimental error, indicating that there is no significant difference of the formal charge between molecules A and B. The donors form conducting sheets, each of which is separated by the insulating layers composed of the anions and solvents (Figure 6). The shortest O−O distance between the neighboring two donor layers is the relatively large value of 6.80 Å. Therefore, strong three-dimensionality is not unfortunately expected for this system. The ET−PDT molecules form a face-to-face stack with a four-folded period as A′ABB′ in which the molecules A−A′ (B−B′) are related to each other with a center of inversion, respectively (Figure 7). The donors are stacked in a head-to-tail manner for molecules AA′ and BB′, whereas they are stacked in a head-to-head manner for AB (Figure 8). All of the overlap modes in the stack are the so-called ring-over-bond type, and the slip distances along the donor long axis are 1.4, 1.7, and 1.2 Å for A−A′, A−B, and B−B′, respectively. The array of donors is close to the so-called β-type array, which is one of the most typical arrangements for the cation radical salts based on TTF donors, and some BEDT−TTF salts, β-(BEDT−TTF)$_2$X (X = I_3, IBr_2 and AuI_2), are known to show superconductivity at low temperatures (T_c = 1.5−8 K).[35] In the case of β-BEDT−TTF salts, the donors form a dimerized column. In contrast, the present salt has a tetramerized stack of donors because there are two crystallographically independent ET−PDT molecules in a column. Therefore, the array of the donors of this salt has a greater resemblance to that of λ-(BETS)$_2$GaCl$_4$,

(35) (a) Kaminskii, V. F.; Prokhorova, T. G.; Shibaeva, R. P.; Yagubskii, E. B. *Pis'ma Zh. Eksp. Teor. Fiz.* **1984**, *39*, 15−18; *JETP. Lett. (Engl. Transl.)* **1984**, *39*, 17−20. (b) Murata, K.; Tokumoto, M.; Anzai, H.; Bando, H.; Saito, G.; Kajimura, K.; Ishiguro, T. *J. Phys. Soc. Jpn.* **1985**, *54*, 1236−1239. (c) Wang, H. H.; Beno, M. A.; Emge, T. J.; Geiser, U.; Firestone, M. A.; Webb, K. S.; Nuñez, L.; Crabtree, G. W.; Carlson, K. D.; Williams, J. M.; Azevedo, L. J.; Kwak, J. F.; Schirber, J. E. *Inorg. Chem.* **1985**, *24*, 2465−2466. (d) Williams, J. M.; Wang, H. H.; Beno, M. A.; Emge, T. J.; Sowa, L. M.; Copps, P. T.; Behroozi, F.; Hall, L. N.; Carlson, K. D.; Crabtree, G. W. *Inorg. Chem.* **1984**, *23*, 3839−3841.

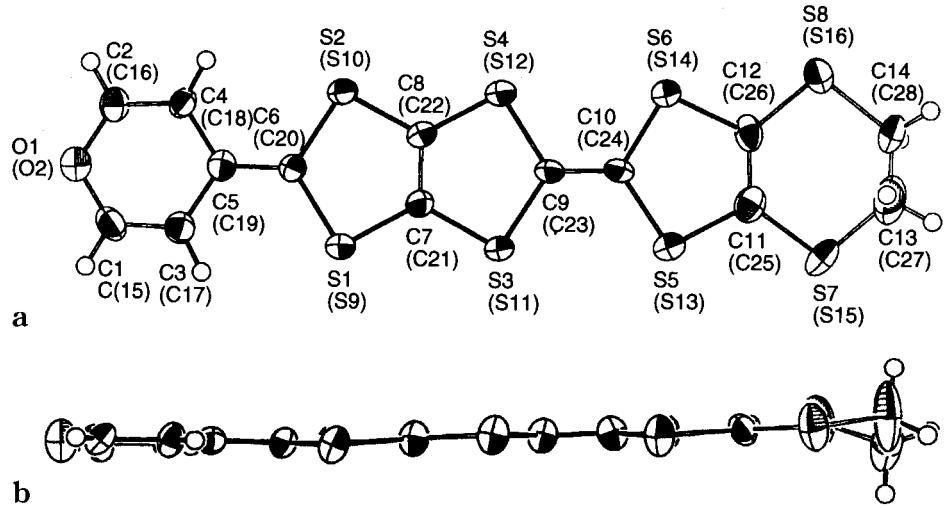

Figure 5. (a) ORTEP drawing and atomic numbering scheme of molecule A and (b) side view of $(ET-PDT)_4PF_6(cn)$. The corresponding atomic numbering scheme of the molecule B is given in parentheses.

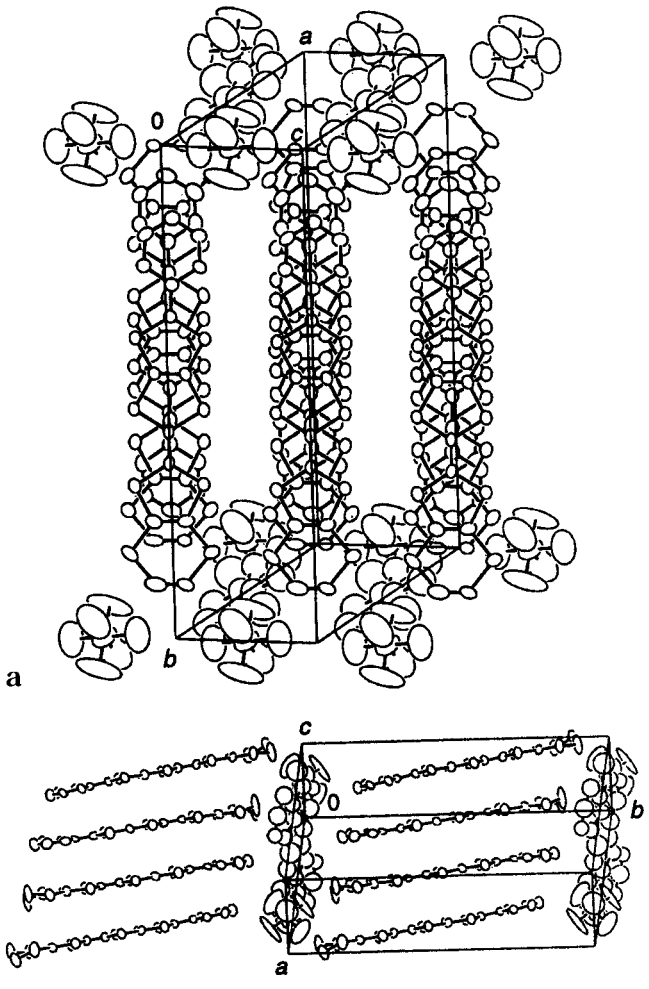

Figure 6. (a) Crystal structure of $(ET-PDT)_4PF_6(cn)$ projected along the stacking direction and (b) projected along the molecular short axis.

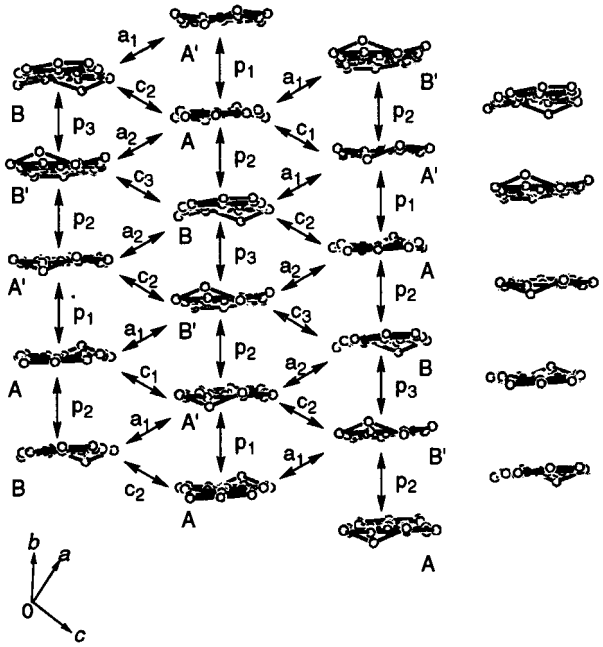

Figure 7. Donor sheet structure of $(ET-PDT)_4PF_6(cn)$. Projection along the molecular long axis. The intermolecular overlap integrals are p1 = 8.6, p2 = −16.4, p3 = 4.9, a1 = 4.4, a2 = 1.5, c1 = 1.7, c2 = −4.5, and c3 = 1.8 ($\times 10^{-3}$).

which is a superconductor with $T_c = 8$ K at ambient pressure.[36] A similar structure was also observed in $(CPTM-TTP)_4X$ (X = PF_6, AsF_6, SbF_6), where CPTM−TTP is 4,5-cyclopenteno-4′,5′-bis(methylthio)-TTP.[37] The interplanar distances of $(ET-PDT)_4PF_6(cn)$ are 3.60, 3.60, and 3.62 Å for A−A′ (p1), A−B (p2), and B−B′ (p3), respectively. The difference of the interplanar distances in the stack (0.02 Å) is much smaller than those for $(CPTM-TTP)_4PF_6$ (0.13 Å) and β-$(BEDT-TTF)_2I_3$ (0.11 Å), suggesting that $(ET-PDT)_4PF_6(cn)$ has an almost uniform stack at first glance.

The overlap integrals were calculated for the adjacent molecules shown by arrows in Figure 7 on the basis of the extended Hückel method (see Supporting Information). A tight-binding band calculation was performed using these overlap integrals.[38] In the present salt, the

(36) Kobayashi, H.; Udagawa, T.; Tomita, H.; Bun, K.; Naito, T.; Kobayashi, A. *Chem. Lett.* **1993**, 1559−1562.

(37) (a) Kawamoto, T.; Mori, T.; Misaki, Y.; Kawakami, K.; Fujiwara, H.; Yamabe, T.; Mori, H.; Tanaka, S. *Mol. Cryst. Liq. Cryst.* **1996**, *284*, 259−270. (b) Misaki, Y.; Kawakami, K.; Fujiwara, H.; Miura, T.; Kochi, T.; Taniguchi, M.; Yamabe, T.; Mori, T.; Mori, H.; Tanaka, S. *Mol. Cryst. Liq. Cryst.* **1997**, *296*, 77−95.

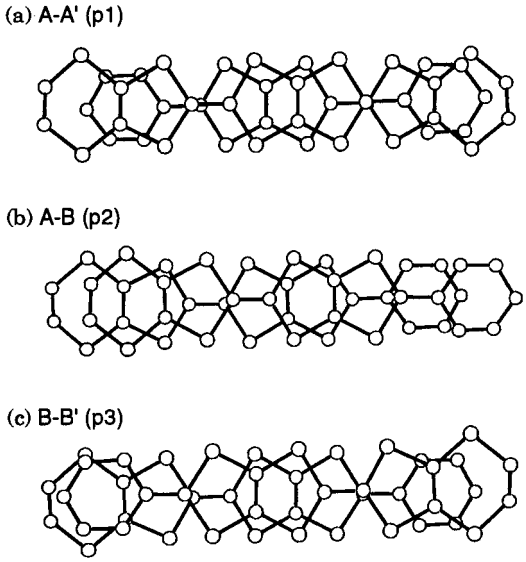

Figure 8. (a) Overlap modes of the donor molecules A−A′ (p1), (b) A−B (p2), and (c) B−B′ (p3) in $(ET-PDT)_4PF_6(cn)$. Projection onto the molecular planes is shown.

head-to-tail overlap prevents an effective intrastack overlap due to the unsymmetrical π-electron framework of PDT−TTP; that is, the phases of the atomic coefficients between the outer 1,3-dithiole ring and the pyran ring are less consistent with each other compared with those between two 1,3-dithioles. In fact, the calculated overlap integrals of the head-to-tail stack, p1 (8.6×10^{-3}) and p3 (4.9×10^{-3}), are only about one-half or a one-fourth of the head-to-head overlap p2 (-16.4×10^{-3}). Therefore, the present salt should be regarded as having a strongly dimerized electronic structure along the stack direction though it seems to have an almost uniform stack from the viewpoint of interplanar distances. Such a difference in the overlap manner does not affect the overlap integrals in $(CPTM-TTP)_4PF_6$ ($19.7-21.3 \times 10^{-3}$), having a symmetrical π-electron framework of TTP.[37a] On the other hand, overlap integrals a1 (4.4×10^{-3}) and c2 (-4.5×10^{-3}) are relatively large, which are about one-fourth of the largest overlaps. Such relatively large interstack overlap integrals are coupled with the largest intrastack overlap integral p2 rather than p1 and p3 (Figure 9). Therefore, the overlap along the *c* direction is much larger than that along the *a* direction. Figure 10 shows the calculated band structure and Fermi surface. A unit cell contains four donor molecules, resulting in the formation of four bands from the HOMO of ET−PDT. A strong dimerization along the stack makes these four bands splitting into two pairs of energy bands (upper and lower bands). The energy gap between the upper and lower bands is 0.06 eV. As a result, the upper bands are three-fourths filled considering that the present salt has a 4:1 composition of donor and anion. Because the overlap along the *c* direction is much larger than that along the *a* direction as mentioned above, the Fermi surface of the present salt is open along the *a* direction.

Magnetic Properties of $(ET-PDT)_4PF_6(cn)$. The static magnetic susceptibility of the $(ET-PDT)_4PF_6(cn)$ was measured on a SQUID magnetometer at 1 T. The

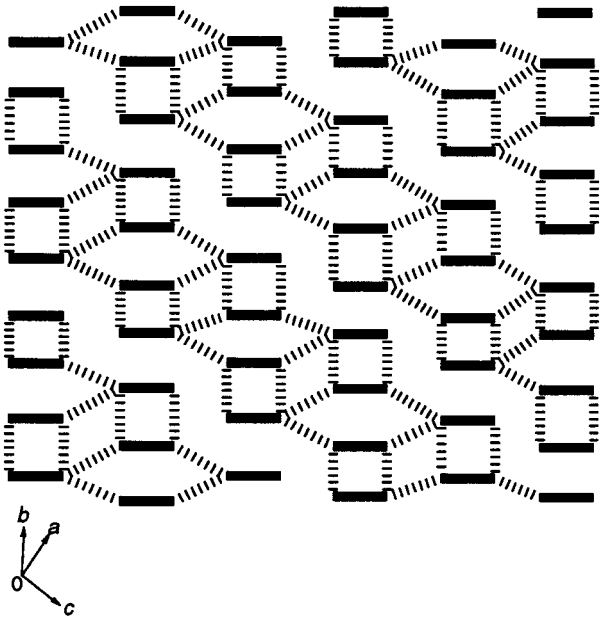

Figure 9. Schematic drawing of overlaps between donor molecules in $(ET-PDT)_4PF_6(cn)$. Bars and broken lines denote the donor molecules projected along the molecular long axis, and relatively large intra- and interstack interactions, respectively.

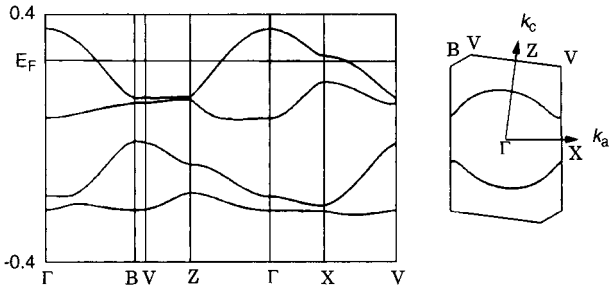

Figure 10. Energy band structure and Fermi surface of $(ET-PDT)_4PF_6(cn)$.

room-temperature susceptibility after the correction of diamagnetic contribution and Curie impurity is 7.0×10^{-4} emu/mol and is slightly larger than that of the normal metallic material, probably due to the large electron correlation derived from the strongly dimerized electronic structure along the stack direction. The temperature dependence of the susceptibility is shown in Figure 11. The magnetic susceptibility is almost temperature-independent down to about 50 K, indicating the Pauli paramagnetism is in correspondence with the metallic conducting behavior down to low temperatures. Though the susceptibility increases a little at low-temperature region, we think that the degree of this increase is very small and this may be derived from the spin localization by the lattice defect. The ESR spectra of the PF_6^- salt were measured on a single crystal with the static magnetic field applied parallel to the crystal plane (parallel to the *ac* plane). The peak-to-peak line width (ΔH_{pp}) and *g* value are $\Delta H_{pp} = 7.3$ G and $g = 2.009$ at room temperature, respectively. This ΔH_{pp} value is rather narrow in comparison with the values for the other β-type salts $(BDT-TTP)_2ClO_4$ (14G)[21b] and $(BEDT-TTF)_2I_3$ (17−23 G),[39] suggesting the relatively

(38) Mori, T.; Kobayashi, A.; Sasaki, Y.; Kobayashi, H.; Saito, G.; Inokuchi, H. *Bull. Chem. Soc. Jpn.* **1984**, *57*, 627−633.

(39) Sugano, T.; Saito, G.; Kinoshita, M.; *Phys. Rev. B: Condens. Matter* **1986**, *34*, 117−125.

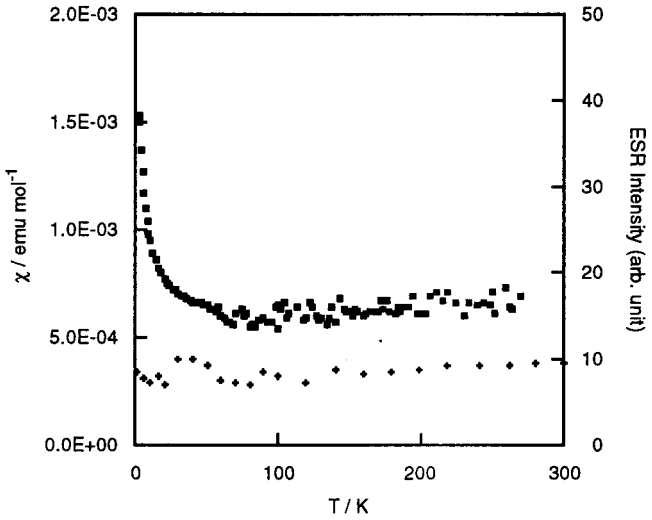

Figure 11. Temperature dependence of static magnetic susceptibility and ESR intensities of $(ET-PDT)_4PF_6(cn)$: (filled squares) magnetic susceptibility; (crosses) ESR intensities.

strong one-dimensional character of the Fermi surface. Variable-temperature ESR measurements have been carried out down to about 2 K to confirm the Pauli paramagnetism of this salt. The *g* values are constant throughout the entire temperature range. The ESR intensities are estimated from the ΔH_{pp} and amplitude (I_m) using the known approximation: intensity $= I_m$-$(\Delta H_{pp})^2$. As also shown in Figure 11, the calculated intensities are almost constant down to 2 K, indicating the Pauli paramagnetism to be the same as in the case of the static magnetic susceptibility measurement. Therefore the PF_6^- salt is observed to sustain its metallic state down to 2 K though the resistivity increased a little at low temperature.

Experimental Section

General Data. THF was freshly distilled under argon over sodium and benzophenone prior to use. Triethyl phosphite was distilled under argon by fractional distillation. Mixed xylene was dried and distilled under argon over CaH_2. Melting points were determined with a Yanaco MP-J3 micro melting point apparatus and not corrected. Microanalyses were performed at the Microanalysis Center, Kyoto University. NMR spectra were recorded on a JEOL FT-NMR Model FX 90Q spectrometer, and chemical shift values are given in parts per million (ppm) relative to internal tetramethylsilane for the ^1H NMR spectra. Mass spectra were obtained with a SHIMADZU Model QP-1000 spectrometer and IR spectra with a BIO-RAD FTS-30 FTIR spectrometer.

2-(Tetrahydropyran-4-ylidene)-1,3,4,6-tetrathiapentalene-5-thione (5). To a stirred solution of 4,5-(diethoxyphosphinylmethylenedithio)-1,3-dithiole-2-thione (**3**) (1.00 g, 2.90 mmol) and tetrahydropyran-4-one (**4**) (318 mg, 3.18 mmol) in 100 mL of dry THF was added dropwise 0.5 M LDA (5.80 mL, 2.90 mmol) for 20 min at −78 °C under argon. The resultant precipitate was filtered and washed with water and then with MeOH and dried in vacuo. The THF filtrate was directly column chromatographed on silica gel with dichloromethane as the eluent and evaporated. The residue was column chromatographed again on silica gel with CS_2 as the eluent. Compound **5** (723 mg, 2.47 mmol) was totally obtained as yellow microcrystals in 86% yield: mp 186−187 °C dec; IR (KBr) ν (cm^{-1}) 1598, 1490, 1462, 1380, 1249, 1094, 1070, 1009, and 965; ^1H NMR (CS_2−C_6D_6, 90 MHz) δ 3.40 (t, $J = 5.4$ Hz, 4H), 1.94 (t, $J = 5.4$ Hz, 4H); MS *m*/*z* 292 (M^+). Anal. Calcd for $C_9H_8OS_5$: C, 36.96; H, 2.76; S, 54.82. Found: C, 36.73; H, 2.89; S, 54.89.

2-(Tetrahydropyran-4-ylidene)-1,3,4,6-tetrathiapentalen-5-one (6). To a solution of **5** (595 mg, 2.04 mmol) in a mixture of chloroform (36 mL) and acetic acid (12 mL) was added mercury(II) acetate (1.11 g, 3.49 mmol) under argon, and the reaction mixture was stirred at room temperature for 2 h. The resultant white precipitate was filtered off and washed with CS_2. The filtrate was washed five times with water to remove acetic acid. The organic layer was dried over sodium sulfate and evaporated. After chromatographic separation on silica gel with CS_2, **6** (513 mg, 1.86 mmol) was obtained as greenish white microcrystals in 91% yield: mp 160−161 °C dec; IR (KBr) ν (cm^{-1}) 1725, 1694, 1589, 1460, 1412, 1333, 1247, 1222, 1089, and 1015; ^1H NMR (CS_2−C_6D_6, 90 M Hz) δ 3.50 (t, $J = 5.4$ Hz, 4H), 2.08 (t, $J = 5.4$ Hz, 4H); MS *m*/*z* 276 (M^+). Anal. Calcd for $C_9H_8O_2S_4$: C, 39.11; H, 2.92; S, 46.40. Found: C, 38.86; H, 2.97; S, 46.66.

2-[4,5-Bis(methoxycarbonyl)-1,3-dithiol-2-ylidene]-5-(tetrahydropyran-4-ylidene)-1,3,4,6-tetrathiapentalene (8b). Compound **6** (200 mg, 0.72 mmol) and 4,5-bis(methoxycarbonyl)-1,3-dithiole-2-thione (**7b**) (362 mg, 1.45 mmol) were stirred in triethyl phosphite (20 mL) at 80 °C under argon for 2 h. After the reaction mixture was cooled to room temperature, the resultant brown precipitate was filtered off, washed with *n*-hexane, and then dried in vacuo. Further purification could not be carried out because of its extremely low solubility to the common solvents. Compound **8b** (300 mg, 0.63 mmol) was obtained as a dark brown powder in 87% yield: mp 211−212 °C dec; IR (KBr) ν (cm^{-1}) 1744, 1717, 1576, 1433, 1288, 1246, 1100, and 1029; high-resolution mass spectrum *m*/*z* calcd for $C_{16}H_{14}O_5S_6$ 477.9165, *m*/*z* found 477.9180.

The other derivatives, **8c** and **8d**, were obtained by the similar procedure mentioned above.

2-[4,5-Bis(methylthio)-1,3-dithiol-2-ylidene]-5-(tetrahydropyran-4-ylidene)-1,3,4,6-tetrathiapentalene (8c). 8c was obtained in 50% yield (166 mg, 0.36 mmol) from **6** (200 mg, 0.72 mmol) and **7c** (328 mg, 1.5 mmol) after column chromatography on silica gel with CS_2 to give reddish orange microcrystals: mp 169−170 °C dec; IR (KBr) ν (cm^{-1}) 1416, 1377, 1312, 1246, 1227, 1094, 1010, and 965; ^1H NMR (CS_2−C_6D_6, 90 MHz) δ 3.45 (t, $J = 5.4$ Hz, 4H), 2.18 (s, 6H), 2.00 (t, $J = 5.4$ Hz, 4H); MS *m*/*z* 454 (M^+). Anal. Calcd for $C_{14}H_{14}OS_8$: C, 36.98; H, 3.10; S, 56.40. Found: C, 36.70; H, 3.23; S, 56.46.

2-(4,5-Ethylenedithio-1,3-dithiol-2-ylidene)-5-(tetrahydropyran-4-ylidene)-1,3,4,6-tetrathiapentalene (8d). 8d was obtained in 65% yield (265 mg, 0.59 mmol) from **6** (250 mg, 0.91 mmol) and **7d** (406 mg, 1.81 mmol) after washing thoroughly with CS_2 in order to eliminate bis(ethylenedithio)-tetrathiafulvalene as the homocoupling product of **7d** to give reddish brown microcrystals: mp 204 °C dec; IR (KBr) ν (cm^{-1}) 1680, 1603, 1408, 1292, 1248, 1222, 1094, 1014, and 966; high-resolution mass spectrum *m*/*z* calcd for $C_{14}H_{12}OS_8$ 451.8653, found 451.8637; Anal. Calcd for $C_{14}H_{12}OS_8$: C, 37.14; H, 2.67. Found: C, 37.07; H, 2.72.

2-[4,5-Bis(methoxycarbonyl)-1,3-dithiol-2-ylidene]-5-(pyran-4-ylidene)-1,3,4,6-tetrathiapentalene (1b). A solution of DDQ (384 mg, 1.69 mmol) in mixed xylene (180 mL) was added dropwise for 30 min to a stirred solution of **8b** (289 mg, 0.60 mmol) in mixed xylene (70 mL) at reflux under argon. After additional 10 min, the hot reaction mixture was filtered, and the filtrate was ice-cooled. The resultant precipitate was filtered and washed with acetonitrile and *n*-hexane and dried in vacuo. Compound **1b** (255 mg, 0.54 mmol) was obtained as brown powder in 90% yield. The analytically pure sample was obtained after recrystallization from chlorobenzene: mp 204−206 °C dec; IR (KBr) ν (cm^{-1}) 1777, 1741, 1714, 1666, 1576, 1430, 1257, 1214, 1082, and 1035; high-resolution mass spectrum *m*/*z* calcd for $C_{16}H_{10}O_5S_6$ 473.8852, found 473.8820.

The other derivatives, **1c** and **1d**, were obtained by the similar procedure mentioned above.

2-[4,5-Bis(methylthio)-1,3-dithiol-2-ylidene]-5-(pyran-4-ylidene)-1,3,4,6-tetrathiapentalene (1c). 1c was obtained in 89% yield (145 mg, 0.32 mmol) from **8c** (166 mg, 0.36 mmol) after column chromatography on silica gel with CS_2 as the eluent to give orange platelike crystals: mp 170−171 °C dec;

IR (KBr) ν (cm^{-1}) 1668, 1587, 1510, 1418, 1258, 1217, 1092, and 1035; ^1H NMR ($CS_2-C_6D_6$, 90 MHz) δ 6.24 (d, J = 7.2 Hz, 2H), 5.28 (d, J = 7.2 Hz, 2H), 2.19 (s, 6H); Anal. Calcd for $C_{14}H_{10}OS_8$: C, 37.31; H, 2.24; S, 56.90. Found: C, 37.01; H, 2.28; S, 57.09.

2-(4,5-Ethylenedithio-1,3-dithiol-2-ylidene)-5-(pyran-4-ylidene)-1,3,4,6-tetrathiapentalene (1d). 1d was obtained in 59% yield from **8d** after column chromatography with hot CS_2 as the eluent to give yellowish brown microcrystals: mp 170−171 °C dec; IR (KBr) ν (cm^{-1}) 1666, 1450, 1379, 1256, 1212, and 1035; high-resolution mass spectrum m/z calcd for $C_{14}H_8OS_8$ 447.8340, found 447.8329.

2-(1,3-Dithiol-2-ylidene)-5-(pyran-4-ylidene)-1,3,4,6-tetrathiapentalene (1a). A mixture of **1b** (100 mg, 0.21 mmol) and $LiBr\cdot H_2O$ (221 mg, 2.1 mmol) in HMPA (35 mL) was held under vacuum with stirring for 1 h to eliminate the trace of amines in the solvent. The mixture was stirred at 90 °C for 1 h and then at 110 °C for 40 min under bubbling argon gas. The reaction mixture was cooled to room temperature and extracted three times with benzene. The organic layer was washed three times with distilled water and dried over sodium sulfate, and the solvent was evaporated in vacuo. The residue was column chromatographed on silica gel with CS_2 as the eluent and recrystallized from chlorobenzene to afford **1a** (66 mg, 0.19 mmol) as orange microcrystals in 88% yield: mp 180−181 °C dec; IR (KBr) ν (cm^{-1}) 1665, 1584, 1560, 1524, 1256, 1214, and 1032; ^1H NMR ($CS_2-C_6D_6$, 90 MHz) δ 6.24 (d, J = 7.2 Hz, 2H), 5.90 (s, 2H), 5.27 (d, J = 7.2 Hz, 2H); MS m/z 358 (M^+); high-resolution mass spectrum m/z calcd for $C_{12}H_6OS_6$ 357.8743, found 357.8731; Anal. Calcd for $C_{12}H_6OS_6$: C, 40.20; H, 1.69. Found: C, 40.30; H, 1.96.

General Procedure for Preparation of TCNQ Complexes and I_3^- Salts. Hot solutions of donor molecule and TCNQ or tetra-*n*-butylammonium triiodide in chlorobenzene were mixed, and the resultant precipitate was collected by filtration. The TCNQ complex was washed with CS_2 and CH_3CN and dried in vacuo. The I_3^- salt was washed with CS_2 and MeOH, and dried in vacuo. The ratio of donor and TCNQ or I_3^- was determined by elemental analysis.

General Procedure for Preparation of Cation Radical Salts. Cation radical salts of **1a,c,d** were prepared by electrochemical oxidation in chlorobenzene−ethanol or 1,2-dichloroethane−ethanol (17:1, v/v) or 1-chloronaphtalene−1,2-dichloroethane−ethanol (8:8:1, v/v) at a constant current of 0.1−0.5 μA in the presence of the corresponding tetra-*n*-butylammonium salts at 20 °C for **1a**,**c** and at 50 °C for **1d** for 1−3 weeks. The crystals obtained were washed with EtOH and were air-dried at room temperature. The ratio of donor and anion was determined by elemental analysis or energy dispersion spectroscopy (EDS).

X-ray Diffractional Analysis of (ET−PDT)$_4$PF$_6$(cn). Crystal data: $C_{66}F_6H_{39}O_4PS_{32}Cl$, M = 2102.37, triclinic, space group $P\bar{1}$, a = 11.656(1) Å, b = 21.561(2) Å, c = 7.9910(9) Å, α = 94.813(9)°, β = 96.251(9)°, γ = 100.001(8)°, V = 1955.1(4) Å^3, Z = 1, D_c = 1.785 g cm^{-3}, μ = 9.88 cm^{-1}, $F(000)$ = 1065.00. A black plate crystal of dimensions 0.60 × 0.17 × 0.04 mm was used for the X-ray measurement at 293 K on a Rigaku AFC7R diffractometer equipped with graphite monochromated Mo Kα radiation (λ = 0.710 69 Å) and a 12 kW rotating anode generator. Cell constants were determined from 25 carefully centered reflections in the range $34.9 < 2\theta < 37.8°$. Intensity data were collected to a maximum 2θ value of 60° by the $\omega-2\theta$ scan technique with scan speed of 16.0°/min. The total number of independent reflections measured was 11 418, of which 4299 were considered to be observed [$I > 2.0\sigma(I)$]. The structure was solved by a direct method (SHELXS86).[40] The non-hydrogen atoms were refined anisotropically except for those of 1-chloronaphthalene, which were refined isotropically. Hydrogen atoms were included but not refined. The structure was refined by full-matrix least-squares methods to R = 0.089, R_w = 0.075, and GOF = 2.74.

Electrochemical Measurement. The cyclic voltammetry system used in this experiment was composed of a Yanaco polarographic analyzer Model P-1100 and a Graphtec X-Y recorder Model WX-1200. The measurement was performed in benzonitrile containing 0.1 M tetra-*n*-butylammonium perchlorate as a supporting electrolyte by use of platinum working and counter electrodes, and a Yanaco saturated calomel electrode (SCE) Model MR-P2A as reference electrode (scan rate: 50 mV/s).

Electrical Conductivity Measurement. Electrical conductivity with the four-probe method was measured by using a Huso Electro Chemical System HESS 994 Multichannel 4-terminal conductometer. Electrical contacts were achieved with gold paste.

Static Magnetic Susceptibility. Measurements of magnetic susceptibility were carried out on the warming process using a Quantum Design MPMS-2 SQUID magnetometer at field of 1 T. The data were corrected for the diamagnetic contribution estimated from Pascal's constants [$\chi^{dia} = -9.43 \times 10^{-4}$ emu/mol for (ET−PDT)$_4$PF$_6$(cn)] and Curie impurities (0.7 mol %).

Electron Spin Resonance. Electron spin resonance spectra were measured on a single crystal which was mounted on a cut flat face of Teflon rod using a small amount of silicon grease and was placed in an evacuated quartz tube.

Acknowledgment. This work was partially supported by a Grant-in-Aid for Scientific Research (No. 06243215, No. 07232219 and No. 09640687) from the Ministry of Education, Science, and Culture of Japan. H.F. is indebted to the JSPS Research Fellowships for Young Scientists.

Supporting Information Available: An X-ray crystallographic file, in CIF format, for (ET−PDT)$_4$PF$_6$(cn) and a table showing the intermolecular overlap integrals of the HOMO, S, and the parameters ϕ and D which define the orientation of adjacent molecules in (ET−PDT)$_4$PF$_6$(cn) together with those of (CPTM−TTP)$_4$PF$_6$[37a] and β-(BEDT−TTF)$_2$I$_3$[41]. This material is available free of charge via the Internet at http://pubs.acs.org.

CM981035P

(40) Sheldrick, G. M. *Crystallographic Computing 3*; Oxford University Press: Oxford, U.K., 1985; pp 175−189.

(41) Mori, T.; Kobayashi, A.; Sasaki, Y.; Kobayashi, H.; Saito, G.; Inokuchi, H. *Chem. Lett.* **1984**, 957−960.